Synthesis of Graphene and Graphene Oxide by Microwave Plasma Chemical Vapor Deposition

Mahmoud Gomaa and Gamal Abdel Fattah*

National Institute of laser Enhanced Sciences (NILES), Cairo University, Cairo, Egypt
*gfattah@niles.edu.eg

Abstract: In this work we construct a simple experiment for rapid synthesis of graphene and graphene oxide (GO) sheets using microwave plasma chemical vapor deposition (MWPCVD) which uses a conventional microwave oven operating at frequency of 2.45GHZandwith a power of 700W to produce plasma inside a tube of quartz for 2min and the polyethylene which consist of small beads was used as a carbon source. The graphene and graphene oxide sheets were characterized by different techniques such as Transmission electron microscopy (TEM), X-ray diffraction, Raman spectroscopy, UV-visible Absorption, Photoluminescence and FT-IR spectroscopy. TEM shows that the morphology of graphene suspension in the form of crumpled and folded sheets, X –ray diffraction for graphene shows the presence of a high and small peak around $2\theta=24.56^{o}$ and $2\theta=43.65^{o}$ respectively. Raman spectra indicated the difference between position and shape of peaks, crystal size and intensity ratio of the D to G modes (I_D/I_G) for graphene and graphene oxide. Also the FT-IR of GO exhibits the presence of C=O ($1735cm^{-1}$), O-H ($3425cm^{-1}$), C=C ($1625cm^{-1}$) and C-O ($1078cm^{-1}$). The emission spectra of GO exhibits abroad emission band between 400 to 800nm. An absorption peak of GO at 235 nm was observed in UV- vis absorption spectra. All the characteristic techniques revealed that MWPCVD is appropriate for synthesis of graphene and graphene oxide.
[Mahmoud Gomaa and Gamal Abdel Fattah. **Synthesis of graphene and graphene oxide by microwave plasma chemical vapor deposition.** *J Am Sci* 2016;12(3):72-80]. ISSN 1545-1003 (print); ISSN 2375-7264 (online). http://www.jofamericanscience.org. 10. doi:10.7537/marsjas12031610.

Keywords: Graphene, Graphene Oxide, Microwave Plasma, polyethylene.

1. Introduction

Graphene is a material discovered by a team out of the University of Manchester in 2004. It is a two-dimensional monolayer of carbon atoms tightly packed into a honeycomb lattice composed of two equivalent sublattices of carbon atoms bonded together with double electron bonds (sp2 bond) in a thin film only one atom thick [1,2]. Graphene which has a hexagonal arrangement of carbon atoms forming one atom thick layer of the layered mineral graphite is a promising material for future electronic applications because of its high electrical conductivity as well as its chemical and physical stability. It serves as the building block of all graphitic materials that can be wrapped up as fullerenes (0D), rolled as nanotubes (1D) and stacked as graphite(3D)[1].There arethree different types of graphene namely single layer graphene (SLG), bi layer graphene (BLG) and few layer graphene (FLG with number of layers (n)≤10)[3] being characterized by its thickness [4]. Several typical methods have been developed for synthesis of graphene such as mechanical exfoliation from highly oriented pyrolytic graphite (HOPG) [5], chemical exfoliation from bulk graphite [6], epitaxial growth on an electrically insulating surface [7], chemical vapor deposition (CVD) [8-10] and the reduction of graphene oxide [11].

In this work chemical vapor deposition (CVD) technique was used to grow graphene and graphene oxide. Generally in chemical vapor deposition the reactant gases are introduced into a reaction chamber and are decomposed and reacted at a heated surface to form the thin film, producing high purity and high performance solid materials [12]. There is different types of chemical vapor deposition such as plasma enhanced chemical vapor deposition (PECVD) which was used in this research, and served as one of early methods for the production of diamond. It forms a few layers of vertically standing graphene and carbon nano walls and enables their deposition at lower temperatures in contrast to traditional CVD which uses higher temperatures to cause the reaction. In PECVD the plasma can be used to accelerate thermodynamical chemical reactions without a catalyst produce and forming films with good adhesion and uniformity [13-15]. Vertical layered graphene has been grown using different methods of PECVD employing microwave plasma, Radio frequency, Arc discharge or electron beam excited plasma where the substrates were exposed to the plasma [13-15].

An easy, fast and straight forward method to synthesize graphene and graphene oxide sheets called microwave plasma chemical vapor deposition (MWPCVD) is present in this work. The method represents a useful and simple batch version of the PCVD technique using polyethylene as a carbon source which can be performed by using a microwave source without the need for a catalyst. MWPCVD is also capable of depositing graphene and graphene

oxide thin films on appropriate surfaces. Graphene oxide is a layer of graphene with oxygen atoms, COOH groups and OH groups attached to it; MWPCVD serves as the most promising precursor for production of graphene and it does not have a completely planar shape due to the addition of oxygen atoms on the top and bottom of carbon layer. The structure of graphene oxide contains epoxide functional groups along the basal plane of sheets as well as hydroxyl and carboxyl moieties along the edges. The graphene oxidized by the addition of C-O-C (epoxide) and C-OH (hydroxyl) groups, the degree of oxidation alters the electronic properties and higher oxidation means the greater band gap.

Both graphene oxide (GO) and reduced graphene oxide (rGO) are used to describe oxidized graphene but with the difference of higher and lower degree of oxidation respectively. This means that reduced graphene oxide (rGO) does not refer to graphene although one of the methods of creating graphene involves the reduction of graphene oxide. Graphene oxide consist of a mixture of sp^3 and sp^2 carbon atoms, the sp^3carbon atoms are bound to the adjacent oxygen containing functional groups while the sp^2 carbon atoms are only connected to the adjacent carbon atoms [16, 17]. The sp^2/sp^3 carbon atomic ratio can vary the PL emission from visible to near–IR wavelength, transforming graphene oxide from an insulator to a semiconductor and tune the band gab of GO [18]. The most common method for synthesizing graphene oxide is the Hummers 'method (oxidation with $KMnO_4$ and $NaNO_3$ in concentrated H_2SO_4) which requires large amount of reagents and along reaction time.

In this work a new method is developed for rapid synthesis of graphene and graphene oxide simultaneously by microwave plasma. Graphene is deposited as black product on the wall of quartz tube, under the plasma ball region and graphene oxide is deposited as yellow product on the wall of quartz tube away from the plasma ball or outside waveguide. Also the graphen and graphen oxide are deposited on appropriate surfaces which were placed under the plasma ball and away from plasma ball respectively.

2. Experimental

The schematic diagram of the MWPCVD set up is shown in figure1. The MWPCVD set up consist of a microwave source operating at 2.45GHZ with maximum power of 700W. The magnetron antenna transmit the microwave energy to the waveguide (length = 30cm). The microwaves are directed to the quartz tube. A quartz tube of 30 cm in length, 2.5cm in diameter and 0.5 cm in thickness was utilized as discharge tube. The polyethylene in the form of small beads was used as carbon source and an aluminum foil cut as a small sheet of $0.5x0.5cm^2$ was used as the trigger for starting plasma. The polyethylene and aluminum foil were put inside the center of the quartz tube and waveguide. The quartz tube was evacuated by a rotary pump for 30 min, and was exposed to microwave irradiation with a power of 700W for 2 min. After the microwave plasma power was switched off, the tube was left for 20 min under vacuum to cool down to room temperature.

The resultant materials were formed as black soot (graphene) on the tube wall inside the waveguide and as yellow color (graphene oxide) on the tube wall outside the waveguide. In order to collect the black soot, the tube was filled with ethanol and shaken for 10 min to allow all of the particles to be dispersed in the solvent (graphene suspension). The yellow color is difficult to remove from the tube wall. Graphene suspension is shown in figure (2.a).

Also by MWPCVD the graphene oxide (yellow color) and graphene (black color) were deposited on appropriate surfaces, two substrates are used, the first substrate is located at 1 cm from the center of the quartz tube inside the waveguide and the second substrate is located outside the waveguide at 3cm from the first substrate. Graphene (black) deposited on the substrate inside the waveguide and graphene oxide (yellow) deposited on the substrate outside the waveguide as in figure2(b, c), then the two samples and the sample of graphene suspension were characterized by different techniques such as TEM, XRD, Raman, UV-visible absorption, photoluminescence and FTR spectroscopy.

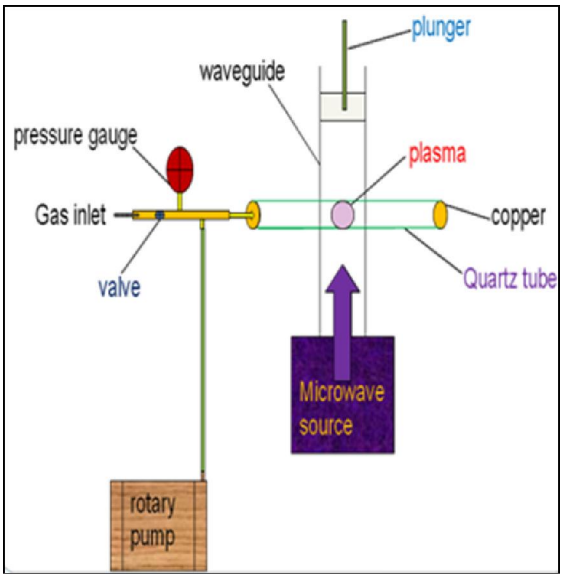

Fig. 1.Schematic diagram of the set up used for synthesis of graphene and graphene oxide by MWPCVD.

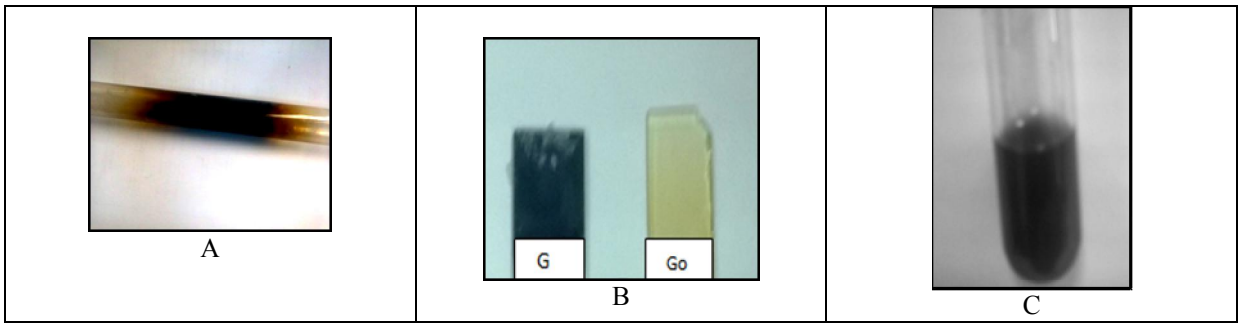

Fig.2. The image of (A) quartz tube after deposition, (B) grapheme G and graphene oxide films on quartz and (C) graphene suspension after shacked process.

The atomic emission spectra of the plasma were collected by an optical fiber into optical spectrometers during deposition. The spectra were measured in the range from 200nm to 800nm during the deposition and the major spectral features are the oxygen ion lines as shown in figure 3. The emission lines in the spectrum have different intensities and are labeled and identified by using NIST data as shown in table 1.

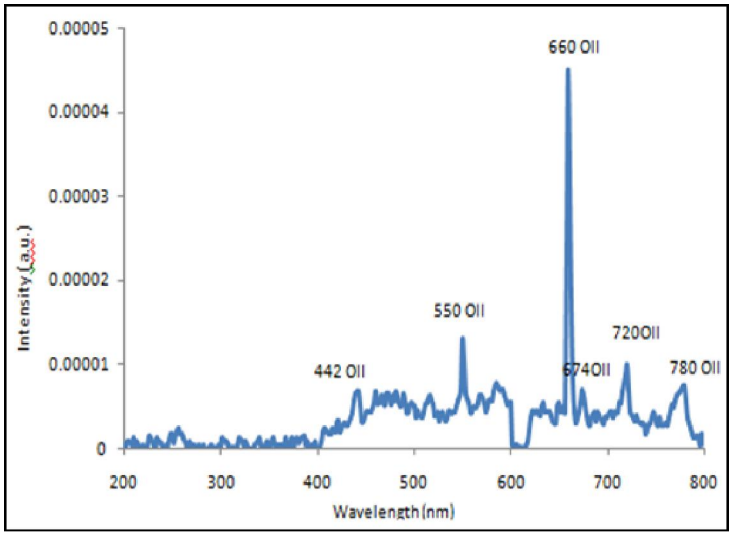

Fig. 3. The optical spectrum of plasma.

Table 1. Emission lines and the corresponding elements of plasma spectrum.

elements	Intensity (a.u.)	Wavelength (nm)
OII	0.68×10^{-5}	442
OII	$1.310\times^{-5}$	550
OII	4.5×10^{-5}	660
OII	0.7×10^{-5}	674
OII	1×10^{-5}	720
OII	0.75×10^{-5}	780

2.1.Characterization.

The x-ray diffraction (XRD) analysis was performed using an X' Pert Pro system with Cu-K_α radiation (λ =1.54060Å), operating at 40 kVand 40 mA to determine the crystal structure and orientation of the sample. For morphological analysis of the sample a two 2-5 µl drops of the prepared dispersion was dried over a 400 mesh copper grid with a holey support film and analyzed using transmission electron microscope JEOL (JEM-1400 TEM). Additional structural information was obtained by Raman spectroscopy [using a laser beam of 532 nm wavelength]. Photoluminescence were obtained by Spectrofluorometer. Fourier Transform Infrared spectra were obtained by FT-IR spectrophotometer in the 4000-1000cm^{-1} region and UV-Vis absorption spectra were obtained by UV-Vis spectrophotometer.

3. Results and discussion.

3.1. X-ray Diffraction

Fig.4. shows the x-ray diffraction pattern of graphene powder (black product) which was collected from the tube wall as black suspension after filling the tube with ethanol and shaken for 20 min, then by allowing the ethanol to evaporate the solution becomes slurry and by dryingit becomes powder. The XRD pattern consists of a two broad peaks, a high peak around ($2\theta = 24.56^{o}$) with d-spacing ($d=3.621A^{o}$) and a small peak around ($2\theta = 43.65^{o}$) with d-spacing ($d=2.0734A^{o}$) which refer to the formation of graphene. Also the figure shows that there is some impurities which are due to the residues of the used materials.

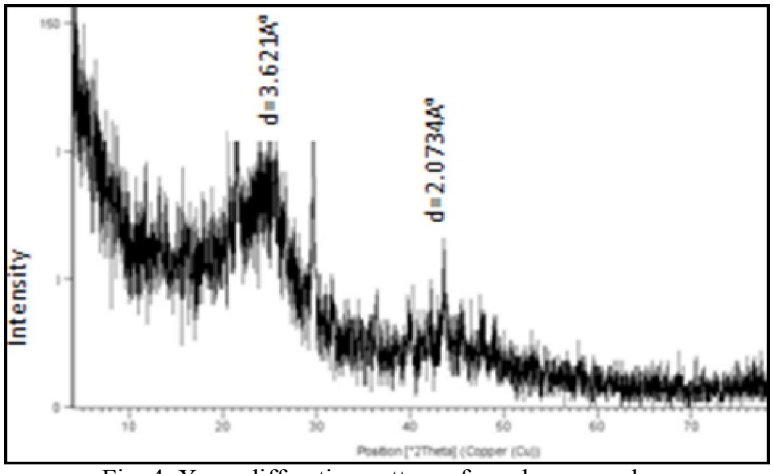

Fig. 4. X-ray diffraction pattern of graphene powder.

3.2. Transmission Electron Microscopy(TEM).

Transmission electron microscopy [TEM] images of our suspended graphene prepared by MWPCVD using polyethylene as carbon source are shown Fig.5. (a, b). From the TEM images the morphology of our sample appears in the form of crumpled and folded sheets with size scale of several hundred nano meters such that the darkest areas can be attributed to the crumpling regions but the less transparent areas are the result of the folding and overlap of a single sheet or the overlap of multiple sheets. The crumpling and folding is often part of the intrinsic nature of the morphology of graphene sheets according to previous studies [19]. The observation of the edges of the suspended film which always fold back by TEM provides a way to determine the number of layers at multiple locations on the film such that the single layer graphene exhibits only one dark line and for bi layer graphene two dark lines should appear and the difference in the number of layers depends on the different locations of the sample [19]. Our transmission electron microscopy (TEM) studies revealed that suspended graphene sheets are not perfectly flat but exhibit crumpling, folding and consist of multi layers.

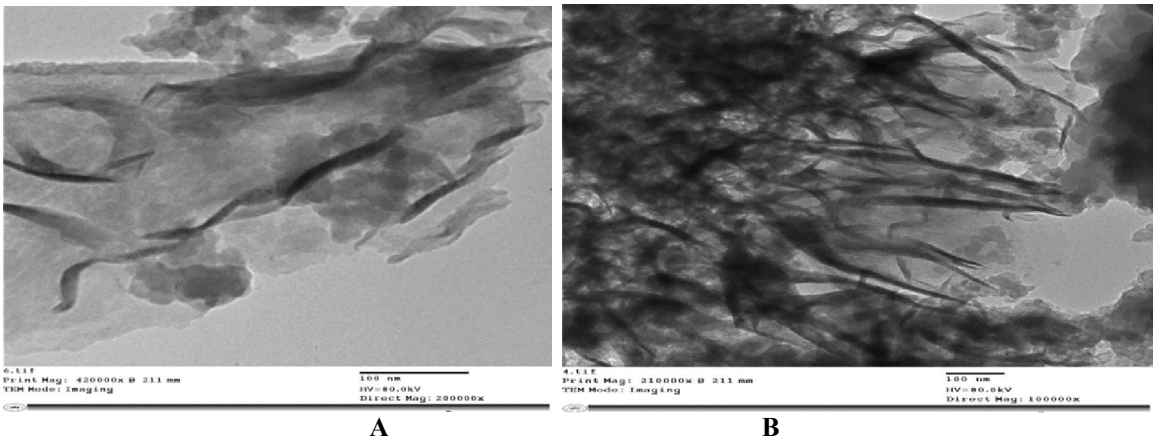

A B

Fig. 5. (A, B). TEM images of graphene nano sheets

3.3. Raman Spectroscopy.

The Raman spectrum of the (graphene suspension) which was prepared by MWPCVD and collected from the wall of tube in ethanol show the two typical peaks of graphitic structures at 1610cm^{-1} labeled as the G band which arises from the zone center of E_{2g} mode and corresponding to ordered sp^2 bonded carbon atoms and the D band at 1332 cm^{-1} which is very weak in graphite and originates from disorder in the sp^2 hybridized carbon atoms as shown in figure6. The Raman spectra of graphene prepared by other methods exhibit a band at 1580 cm^{-1} (G band) and a band at 1350 cm^{-1} (D band) [20]. Our spectrum noted that D band exhibited the greatest intensity and G band shifted to higher wave numbers (1610cm^{-1}) and this shift is due to the presence of stronger defects in this sample and the thickness of the sample. The intensity ratio of the D to G modes ($I_D/_{IG}$) measures the disorder degree in the sample and average size of the sp^2 domains. The crystal size was estimated according to the D band /G peak intensity ratio by this equation La (nm) = $(2.4\times10^{-10})\ \lambda^4\ (I_D/I_G)^{-1}$which was found by Cancado *et al*. [21, 22]. From the Raman spectra of our suspended graphene the intensity ratio (I_D/I_G) = 0.90 and the crystal size (L_a) = 21 nm. When we compare between these crystallite size result (L_a) = 21nm and the observed size of sheets in the transmission electron microscopy images (several hundred nano meters) it can be concluded that the morphology of the suspended graphene sample involves the overlaying of multiple sheets consisting of around 4-5 graphene layers.

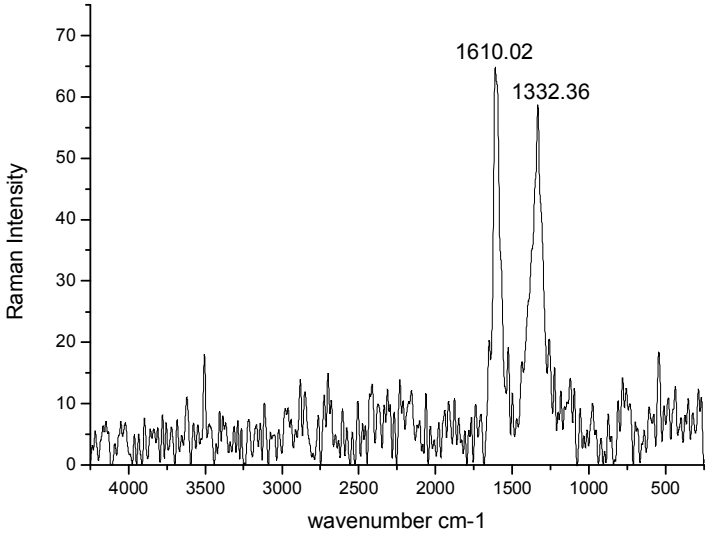

Fig.6. Raman spectra of suspended graphene.

Fig.7. shows the Raman spectra of graphene film which was deposited on a substrate of quartz which was put in the quartz tube inside the waveguide. The Raman spectrum of graphene film on quartz substrate showed G band at 1586cm^{-1}, D band at 1354 cm^{-1}, D\ at 1620 cm^{-1}. The 2D and the disorder induced combination mode (D+G) peaks can also be observed at 2710 and 2949 cm^{-1}. There is a blue shift (5cm^{-1}) in G band position (1586cm^{-1}) when compared to bulk graphite (1581 cm^{-1}) and this shift is attributed to the transformation of bulk graphite crystal to graphene sheets and the 2D band peak is used to confirm the presence of graphene[23]. The number of graphene layers was determined by the position and shape of the 2D band peak such that Single layer graphene sheets have a single sharp 2D peak below 2700cm^{-1}, while bi layer sheets have a broader and up shifted 2D peak located at 2700 cm^{-1}and the sheets with more than Five layers exhibit similar spectra which have broad 2D peaks that are up shifted to position greater than 2700 cm^{-1}[24]. From our Raman spectrum the 2D band peak observed at 2710 cm^{-1} which is greater than 2700 cm^{-1} and this means that our sample consist of multilayer of graphene. Also the intensity ratio of the 2D to G band peaks can be determine the number of graphene layers such that the single layer of graphene can demonstrated if (I_{2D}/I_G) ≥2 otherwise it is bi layers even multi layers, the number of graphene layers decrease with increasing the intensity ratio of (I_{2D}/I_G) [21, 25] and from figure.7.The intensity ratio (I_{2D}/I_G) = 0.25which < 2 and this mean that our sample

consists of multi layers of graphene. According to the resonant Raman scattering theory the intensity of defect bands (I_D, $I_{D\backslash}$) depends on the amount of defects, the type of defects associated with it and the intensity ratio of defect bands ($I_D/I_{D\backslash}$) would provide information about the type of defects present in the material such that if the ratio of ($I_D/I_{D\backslash}$) =13 it indicates the presence of sp^3 related defects, and similarly 10.5 corresponds to hopping defects, 7 for vacancy like defects, 3.5 for boundary like defects and 1.3 represents the one site defects in graphene as reported in previous studies[26] and by applying this information to our spectrum were found that the intensity ratio of defect bands ($I_D/I_{D\backslash}$) = 1.3 this means that the type of defects in our sample represents one site defects in graphene. Also from the Raman spectrum the intensity ratio of the D to G modes (I_D/I_G) = 1.09 and crystal size according to Cancado *et al.* equation (L_a) = 18 nm. From the above it was concluded that our sample is graphene with multi layers.

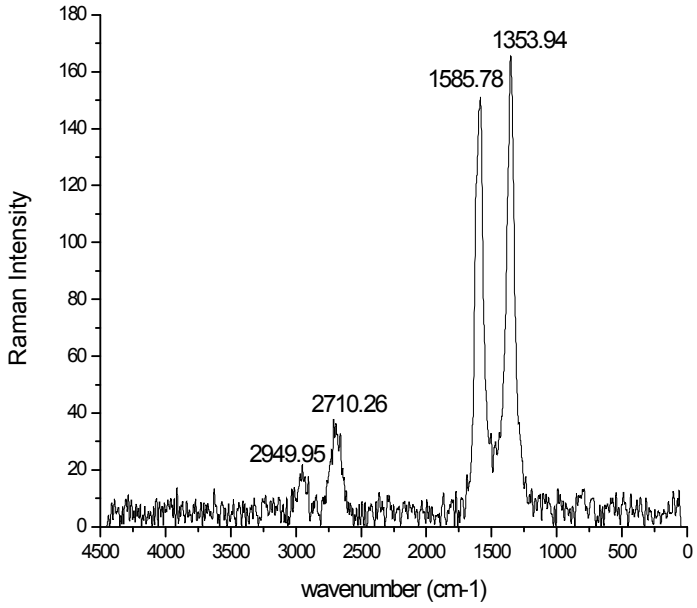

Fig. 7. Raman spectra of graphen film on substrate.

The Raman spectrum of graphene oxide deposited by MWPCVD on a substrate of glass which was put inside the quartz tube outside the waveguide shows the presence of G band at 1616 cm^{-1} and D band at 1342cm^{-1} as shown in fig.(8). From the figure the G band is shifted towards higher wave number which is due to the oxygenation of graphite which results in the formation of sp^3 carbon atoms. The D band is broadened due to the reduction in size of in plane sp^2 domains by the creation of defects vacancies and distortion of the sp^2 domains during oxidation [27]. There is some differences which distinguish between the graphene and graphene oxide such as the intensity ratio (I_D/I_G) of graphene higher than those of graphene oxide, the increase in intensity ratio is attributed to a lower degree of crystallinity in graphitic material and the average crystallite size (L_a) of sp^2 domains is decreased in graphene due to the formation of new sp^2 carbon atoms which are smaller in sizethan the sp^2 carbon atoms present in graphene oxide [28, 29]. From the above information and the Raman spectra of graphene oxide it was found that the intensity ratio of D to G modes (I_D/I_G) = 0.57 which is less than (I_D/ I_G) = 1.09 of graphene in our previous sample (I_D/I_G of this sample < I_D /I_G of graphene) and the crystal size (L_a) of graphene oxide according to Cancado *et al.* equation La = 34 nm which is higher than crystal size (L_a = 18 nm) of graphene in our previous sample (L_a of graphene < L_a of this sample). From all of the above results it was concluded that our sample is graphene oxide.

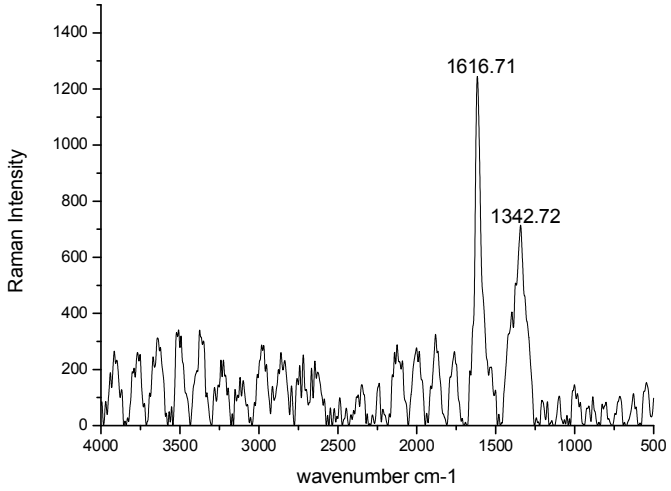

Fig. 8. Raman spectra of graphene oxide film on substrate.

3.4. Spectrofluorometer Analysis.

The figure (9a) shows the fluorescence emission spectra of graphene oxide with different excitation wavelengths (350 – 550nm). From the figure the graphene oxide exhibits abroad emission band between 400 and 800 nm due to its heterogeneous electronic structure and this emission associated with the aromatic C-OH, C=C and COOH functional groups. Also from the figure the positions of emission peaks were dependent on the excitation wavelengths, the maximum of the emission peaks red-shifted to higher wavelengths with increase in the excitation wavelength and these peaks have different relative intensities. When the relation between excitation energy and also emission energy were plotted as in figure (9b), it is obvious that the excitation wavelength versus the emission wavelength.

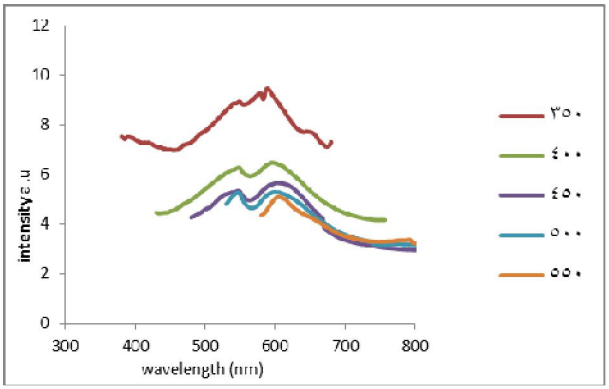

Fig 9a. Emission spectra of graphene oxide.

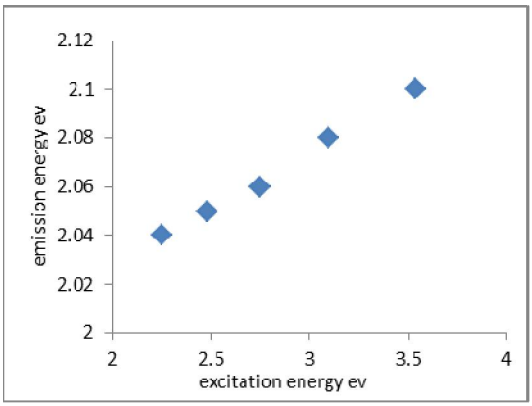

Fig. 9b. Fluorescence emission photon energy maxima versus excitation photon energy.

3.5. FT-IR Analysis.

The FT-IR spectrum of the graphene oxide as in figure10 shows several peaks, a peak at 3425 cm^{-1} originated from (O-H) stretching vibration indicating abroad and intense absorption, the absorption peaks of the alkyl group at 2860 and 2926 cm^{-1} correspond to the symmetric and anti- symmetric stretching vibrations of CH_2, a peak at 1735cm^{-1} due to the (C=O) stretching of carboxylic groups placed at the edges of GO sheets, C-O-C (1196cm^{-1}), C-O (1078cm^{-1}) and a peak at1445 $cm^{-1}$for (O-H). Finally the absorption peak at 1625cm^{-1} can be attributed to in plane C=C bands present at the edges of graphene oxide [30]. From the figure there are strong bands associated with CH_2 groups observed at 2926 and 2860cm^{-1} respectively due to polyethylene which was used as carbon source and the presence of these oxygen containing groups indicated that graphene has been oxidized.

3.6. UV-Visible Spectroscopy.

The absorption spectrum of graphene oxide is shown in fig. (11).The figure shows that the absorption peak for the prepared graphene oxide at 235 nm is considered due to the π -π* (C=C) transition and the smart peaks are due to n→π* transition of C=O. From the absorbance measurements in UV-Vis absorption spectrum the absorption coefficient α of graphene oxide film can be determined; photon energy (hν) can be calculated by hν =1240/λ and the energy gap Eg of graphene oxide is estimated by the following equation $\alpha h\nu = k (h\nu - Eg)^{1/2}$ where k is a constant. When the relation between photon energy (hν) and the coefficient as a function of wave length $(\alpha h\nu)^2$ were plotted, the energy gap Eg of graphene oxide is determined by extrapolating the straight line portion of the spectrum αhν = 0 as in fig. (12). From the figure the value of energy gap (Eg) of graphene oxide = 3.1 ev.

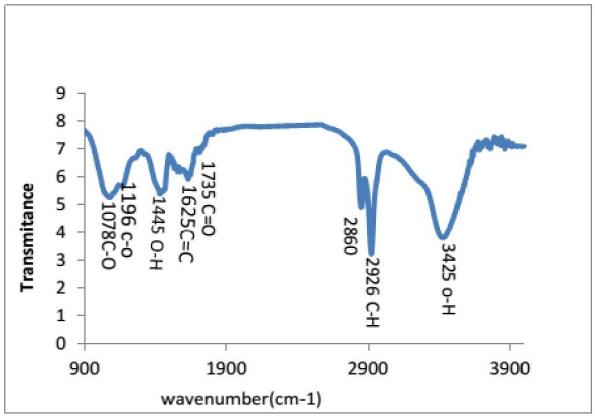

Fig. 10.FT-IR spectra of graphene oxide.

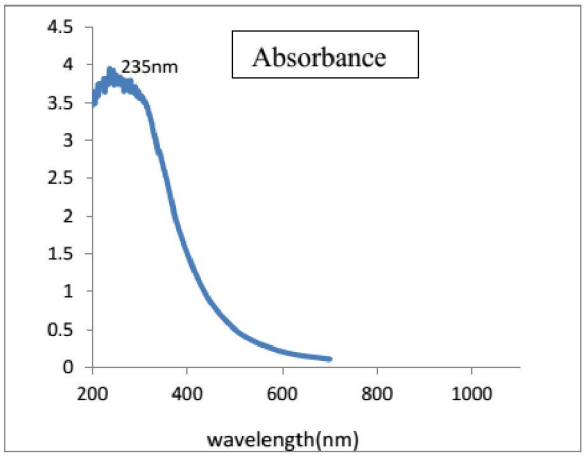

Fig. 11. UV-Vis absorption spectrum of graphene oxide film.

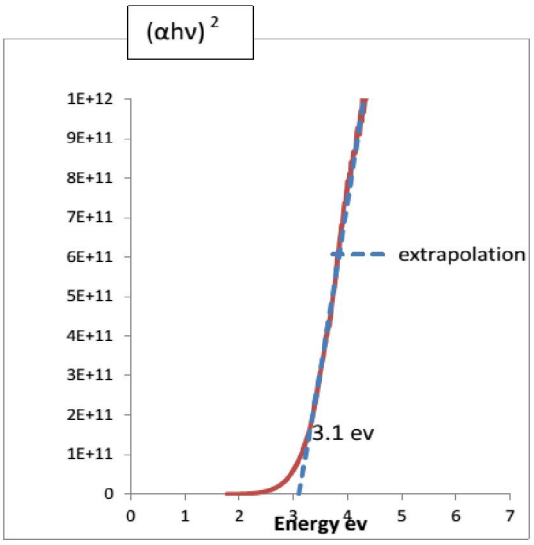

Fig. 12: Measurement of energy gap for graphene oxide film.

3. Conclusion

In this study, a simple experiment was constructed for the synthesis of graphene and graphene oxide by microwave plasma chemical vapor deposition using microwave source operating at 2.45GHZ and with a power of 700W and the polyethylene was used as carbon source instead of other materials which is toxic such as CH_4. Several method have been developed for the synthesis of graphene and graphene oxide which require along reaction time but in MWPCVD the graphene and graphene oxide were synthesized when the quartz tube and polyethylene had exposed to microwave irradiation for 2 min and a power of 700W and the deposited films were good adhesion and uniformity. The deposited samples were characterized by different techniques which distinguished between graphene and graphene oxide and revealed that MWPCVD is appropriate for synthesis of graphene and graphene oxide. The MWPCVD create a new way for the synthesis of graphene and graphene oxide in short time and is safe for the environment.

References

1. Geim. A. K and K. S. Novoselov. The rise of graphene. Nat. Mater 6, 183, (2007).
2. Zhenhua Ni, Y. Wang, T. Yu and Z. Shen. Raman spectroscopy and imaging of graphene. Nano. Res1, 273, (2008).
3. Rao. C. N. R, A. K. Sood, K. S. Subrahmanyam and A.Govindaraj. Graphene: The New Two-Dimensional Nanomaterial. Angew. Chem. Int. Ed 48, 7752, (2009).
4. Wang. Y. Y, Z. H. Ni, Z. X. Shen, H. M. Wang and Y. H. Wu. Probing charged impurities in suspended

graphene using Raman spectroscopy. Appl. Phys. Lett 92, 043121-1, (2008).
5. Novoselov. K. S, A. K. Geim, S. V. Morozov, D. Jiang, Zhang, S. V. Dubonos, I. V. Grigorieva, and A. A. Firsov. Electric field effect in atomically thin carbon films. Science 306,666, (2004).
6. Goki Eda, G. Fanchini, and M. Chhowalla. Large-area ultrathin films of reduced graphene oxide as a transparent and flexible electronic material. Nat. Nanotechnology 3, 270, (2008).
7. Ohta. T, A. Bostwick, T. Seyller, K. Horn, and E. Rotenberg. Controlling the electronic structure of bi-layer graphene. Science 313, 951, (2006).
8. Qingkai. Y, J. Lian, S. Siriponglert, H. Li, Y. P. Chen, and S. S. Pei. Graphene segregated on Ni surfaces and transferred to insulators. Appl. Phys. Lett 93, 113103, (2008).
9. Reina. A, X. Jia, J. Ho, D. Nezich, H. Son, V. Bulovic, M. S. Dresselhaus, and J. Kong. Large area, few-layer graphene films on arbitrary substrates by chemical vapor deposition. Nano Lett 9, 30, (2009).
10. Cecilia Mattevi, H. Kima, and M. Chhowalla. A review of chemical vapour deposition of graphene on copper. J. Mater. Chem 21, 3342, (2011).
11. Daniel R. S. P, Dreyer, Christopher W. Bielawski and and R. S. Ruoff. The chemistry of graphene oxide. CRITICAL REVIEW 39, 228–240 (2009).
12. Terranova M. L, V. Sessa and M. Rossi. The world of carbon nanotubes: An overview of CVD growth methodologies. Chem. Vap.Deposition12, 315, (2006).
13. Wu Y. H, P. W. Qiao, T. C. Chong, and Z. X. Shen. Carbon nanowalls grown by microwave plasma enhanced chemical vapor deposition. Adv. Mater 14, 64, (2002).
14. Wang. J. J, M. Y. Zhu, R. A. Outlaw, X. Zhao, D. M. Manos, B. C. Holloway, and V. P. Mammana. Free-standing subnanometer graphite sheets. Appl. Phys. Lett 85, 1265, (2004).
15. Mori. T, M. Hiramatsu, K. Yamakawa, K. Takeda, and M. Hori: Fabrication of carbon nanowalls using electron beam excited plasma-enhanced chemical vapor deposition. Diamond Relat. Mater 17, 1513, (2008).
16. Eda. G, Y.-Y. Lin, C. Mattevi, H. Yamaguchi, H.-A. Chen,I.-S. Chen, C.-W. Chen and M. Chhowalla. Blue photoluminescence from chemically derived graphene oxide. Adv. Mater 22,505-509, (2010).
17. Chen. J. L, X.-P. Yan, K. Meng and S.-F. Wang. Graphene oxide based photoinduced charge transfer label-free near-infrared fluorescent biosensor for dopamine. Anal. Chem 83, 8787-8793, (2011).
18. Gokus. T, R. R. Nair, A. Bonetti, M. Bo¨hmler, A. Lombardo, K. S. Novoselov, A. K. Geim, A. C. Ferrari and A. Hartschuh. Making Graphene Luminescent by Oxygen Plasma Treatment. ACS Nano 3, 3963-3968, (2009).
19. Meyer JC, Geim AK, Katsnelson MI, Novoselov KS, Booth TJ, Roth S. The structure of suspended graphene sheets. Nature 446(7131), 60, (2007).
20. Ferrari AC, Robertson J. Interpretation of Raman spectra of disordered and amorphous carbon. Phys Rev B 61(20), 14095–107, (2000).
21. Ferrari AC, Meyer JC, Scardaci V, Casiraghi C, Lazzeri M, MauriF, et al. Raman Spectrum of Graphene and Graphene Layers. Phys Rev Lett 97(18), 187401–4, (2006).
22. Pan. D.Y, S. Wang, B. Zhao, M.H. Wu, H.J. Zhang, Y. Wang et al. Li storage properties of disordered graphene nanosheets. Chem Mater 21 (14), 3136–3142, (2009).
23. Pimenta M.A, G. Dresselhaus, M.S. Dresselhaus, L.A. Cancado, A. Jorio, R. Saito. Studying disorder in graphite-based systems by Raman spectroscopy. Phys Chem Chem Phys 9, 1276–1291, (2007).
24. Casiraghi. C, Pisana. S, Novoselov. K. S, Geim. A. K, Ferrari. A. C. Raman fingerprint of charged impurities in graphene. Appl. Phys. Lett 91, 233108, (2007).
25. Kim. K. S, Y. Zhao, H. Jang, S. Y. Lee, J. M. Kim, K. S. Kim, J.-H. Ahn, P. Kim, J.-Y. Choi, and B. H. Hong. Large-scale pattern growth of graphene films for stretchable transparent electrodes. Nature 457, 706, (2009).
26. Eckmann A, Felten A, Mishchenko A, Britnell L, Krupke R, Novoselov K S and Casiraghi C. Probing the nature of defects in graphene by Raman spectroscopy. Nano Lett 12(8), 3925, (2012).
27. Stankovich, S.; Dikin, D. A.; Piner, R. D.; Kohlhaas, K. A.; Kleinhammes, A.; Jia, Y.; Wu, Y.; Nguyen, S. T.; Ruoff, R. S. Synthesis of graphene-based nanosheets via chemical reduction of exfoliated graphite oxide. Carbon 45, 1558-1565, (2007).
28. Chengzhou Zhu, Guo, S.; Fang, Y.; Dong, S. Reducing Sugar: New Functional Molecules for the Green Synthesis of Graphene Nanosheets. ACS Nano 4, 2429-2437, (2010).
29. Krishnamurthy. K, Veerapandian. M, Mohan. R, Kim. S. J. Investigation of Raman and photoluminescence studies of reduced graphene oxide sheets. Appl. Phys. A106, 501-506, (2012).
30. Hui. Lin Guo, X. Wang, Q. Qian, F. Wang, X. Xia. A green approach to the synthesis of graphene nanosheets. ACS Nano 3, 2653-59, (2009).

2/24/2016